Mon. Not. R. Astron. Soc. **000**, 1–16 (2014) Printed 15 September 2014 (MN LATEX style file v2.2)

A high resolution image of the inner-shell of the P Cygni nebula in the infra-red [Fe II] line

C. Arcidiacono[1⋆], R. Ragazzoni[2], C. Morossi[3], M. Franchini[3], P. Di Marcantonio[3], C. Kulesa[4], D. McCarthy[4], R. Briguglio[5], M. Xompero[5], L. Busoni[5], F. Quirós-Pacheco[5], E. Pinna[5], K. Boutsia[6], and D. Paris[6]

[1]*INAF – Osservatorio Astronomico di Bologna, Via Ranzani, 1, I–40127 Bologna, Italy*

[2]*INAF – Osservatorio Astronomico di Padova, Vicolo dell'osservatorio, 5, I–35122 Padova, Italy*

[3]*INAF - Osservatorio Astronomico di Trieste, Via G. B. Tiepolo 11, Trieste, I–34143, Italy*

[4]*Steward Observatory Annex, 1540 East Second Street Tucson, AZ 85721-0064, USA*

[5]*INAF – Osservatorio Astrofisico di Arcetri, Largo Enrico Fermi, 5, I–50125 Firenze, Italy*

[6]*INAF – Osservatorio Astronomico di Roma, Via Frascati, 33, I–00040 Monte Porzio Catone, Italy*

Accepted . Received; in original form

arXiv:1409.3721v1 [astro-ph.SR] 12 Sep 2014

ABSTRACT

We have obtained with the LBT Telescope AO system Near-Infrared camera PISCES images of the inner–shell of the nebula around the luminous blue variable star P Cygni in the [Fe II] emission line at 1.6435 μm. We have combined the images in order to cover a field of view of about 20″ around P Cygni thus providing the high resolution (0″.08) 2–D spatial distribution of the inner–shell of the P Cygni nebula in [Fe II]. We have identified several nebular emission regions which are characterized by an S/N>3. A comparison of our results with those available in the literature shows full consistency with the finding by Smith & Hartigan (2006) which are based on radial velocity measurements and their relatively good agreement with the extension of emission nebula in [N II] λ6584 found by Barlow et al. (1994). We have clearly detected extended emission also inside the radial distance R=7″.8 and outside R=9″.7 which are the nebular boundaries proposed by Smith & Hartigan (2006). New complementary spectroscopic observations to measure radial velocities and to derive the 3–D distribution of P Cygni nebula are planned.

Key words: *(stars): circumstellar matter – stars: individual: P Cygni – instrumentation: adaptive optics.*

1 INTRODUCTION

The star P Cygni was discovered on August 18, 1600 AD when it brightened to about the third magnitude. It is a "prototypical" Galactic Luminous Blue Variable (LBV) star and its basic properties are described by Najarro, Hillier & Stahl (1997) and Najarro (2001).

Several attempts to get informations on size, chemical composition and density distribution of the material around the star have been already done (see for example Latherer & Zickgraf 1987). Barlow et al. (1994) got [N II] λ6584 narrow band images showing unresolved clumps of emission distributed within a nearly circular nebula with angular diameter of about 22″ and hint at the presence of nebular rings with radii of 6″ and 11″. Barlow et al. (1994) found clumps, typically 2″–3″ in diameter, not symmetrically distributed around the star (see Nota, Livio, & Clampin 1995). On the other hand, White & Becker (1982) observations are consistent with a homogeneous, spherically symmetric, constant velocity, isothermal flow. An outer shell with a radius of ∼1′.6 is also present indicating mass ejection before 1600 AD (see for example Meaburn et al. 1996, Meaburn, Lopez & O'Connor, 1999, Meaburn et al. 2004)

Near-InfraRed (NIR) spectroscopy of P Cygni (Smith 2001 and Smith & Hartigan 2006) revealed bright emission in the [Fe II] line at λ=1.6435 μm. Smith & Hartigan (2006) derived from the analysis of high–resolution spectra the following geometric parameters of P Cygni inner–shell: a mean expansion velocity of 136 km s^{-1}, a shell radius of about $10^{17.3}$ cm, a dynamic age of about 530 yr, and a geometric filling factor in [Fe II] roughly equal to 0.2. They concluded that the [Fe II] emitting shell at about 10″ from P Cygni is the product of the 1600 AD outburst. In their results the cause of greater uncertainty was the uncertainty in the adopted P Cygni distance (1.7±0.1 kpc) and the need of assuming a filling factor. In fact, the choice of the latter was somehow arbitrary since they had no NIR images and only relatively low spatial resolutions orthogonally and along their long slit spectra, i.e. ∼ 0″.5 and ∼ 2″, respectively.

A significant step forward in the knowledge of P Cygni nebula in particular and of LBV stars in general would require high resolution 3–D information on the nebular structure which, in our opinion, has become possible with the availability, nowadays, of large ground–based telescopes, technologically advanced instruments, and Adaptive Optics (AO) systems. In this paper we present a collage of 72 Near-Infrared camera PISCES (McCarthy et al. 2001)

⋆ E-mail: carmelo.arcidiacono@oabo.inaf.it (CA)

images obtained by the Large Binocular Telescope (LBT, Hill 2010)[1] AO system in a narrow band filter centered on the 1.6435 μm NIR forbidden line of Fe II. The final image covers a field of view of about 20″ around P Cygni and provides high resolution 2–D information on P Cygni nebula which will be complemented with future radial velocity observations in order to derive the nebular distribution along the line of sight. In Section 2 we present the main characteristics of the instrumental setup and of the acquired AO images; in Section 3 we describe the image processing which lead to a composite image of the nebular emission around P Cygni from the set of 72 individual images; in Section 4 the 2–D spatial distribution of P Cygni nebula is presented and our results are compared with those already available in the literature.

2 OBSERVATIONS

2.1 The Adaptive Optics

Both telescopes of the LBT are equipped with a high order adaptive optics system called First Light Adaptive Optics, FLAO (Esposito et al. 2012). The FLAO senses the atmospheric turbulence by means of a pyramid based wavefront sensor (Ragazzoni 1996) which samples the pupil on a grid of 30×30 sub-apertures. A corrected wavefront is obtained through an Adaptive Secondary Mirror (ASM) (Salinari, del Vecchio & Biliotti 1993 and Riccardi et al. 2010) controlled by 672 actuators at a frequency of 1 kHz. The spatial and temporal configurations of the FLAO match the performance of the ASM. On typical seeing values of 0″.8 the FLAO provides in the H band high order corrected images with Strehl Ratios of about 80% on bright reference sources.

P Cygni is a bright reference for the FLAO system, whose R band magnitude operative range is between 3.5 and the 17 mag. Actually, the FLAO system, whose filter of the wavefront sensor is centered at 0.7μm, detected this star as a 5.5 mag object.

[1] The LBT is an international collaboration among institutions in the United States, Italy and Germany. LBT Corporation partners are: The University of Arizona on behalf of the Arizona university system; Istituto Nazionale di Astrofisica, Italy; LBT Beteiligungsgesellschaft, Germany, representing the Max-Planck Society, the Astrophysical Institute Potsdam, and Heidelberg University; The Ohio State University, and The Research Corporation, on behalf of The University of Notre Dame, University of Minnesota, and University of Virginia.

2.2 PISCES Camera

In order to provide early science with the LBT Adaptive Optics system before the arrival at the telescope of the diffraction limited camera, we have the opportunity to utilize the PISCES infrared camera provided by the University of Arizona. PISCES provides diffraction limited images in the 1–2.5 μm range with a pixelscale of 0.019 arcsec/px. Further details on PISCES camera can be found in McCarthy et al. (2001), Esposito et al. (2013) and Guerra et al. (2012).

2.3 Observing strategy

The observations of P Cygni were obtained on June 22$^{\rm nd}$ 2012 in the [FeII] emission line filter centered on the emission line at 1.6435 μm. In order to avoid saturation and to cover a field of about 46″ in diameter centered on P Cygni, we intentionally moved the star out of the field of view. We used 12 different observational sets: the first four were obtained by putting P Cygni about 0″.5 North, South, East, or West out of the field of view; the other eight set were obtained from the first four after applying a 30 or 60 degrees rotation of the LBT Gregorian Rotator. We took six 20 s images in each observational set leading to a total of 72 images. During the observations the Differential Image Motion Monitor (DIMM) on board the LBT measured a variable seeing between 0″.9 to 1″.5 (V band). The telescope elevation was ranging from 70 to 84 degrees and the DIMM was pointing as close as possible to the target.

3 DATA REDUCTION

We follow a standard data reduction method for near infrared data. Electronic cross–talk between the quadrants in the PISCES detector was corrected using "Corquad", an IRAF[2] procedure developed by Roelof de Jong[3]. The Full Width at Half Maximum (FWHM) of a few stars present in each reduced frame is about 0″.07 -.10″, slightly variable along the field of view because of the anisoplanatism effect. The average FWHM and Strehl Ratio (SR) are 0″.08 and 12%, respectively.

[2] IRAF 2011, "Image Reduction and Analysis Facility", Version 2.15.1a, NOAO, Tucson
[3] See website http://66.194.178.32/∼rfinn/pisces.html)

Table 1. P Cygni nebula emission regions

Region	Size arcsec^2	Tot. Int. counts	Knot #	RA hh:mm:ss	DEC deg : min : sec	Max Int. counts pix^{-1}
A	7.4	62331				
B	1.4	19777	1	20:17:47.7	+38:02:13.9	204[a]
C	1.0	8691				
D	4.8	39952				
E	0.4	3809				
F	4.2	48335				
G	16.3	244982	1	20:17:47.9	+38:01:59.1	17
			2	20:17:47.7	+38:01:56.0	15
H	2.3	20145				
I	1.6	11607				
J	4.8	49098	1	20:17:47.6	+38:01:51.2	13
K	4.6	41238	1	20:17:46.6	+38:01:41.0	126[a]
L	3.3	29458				
M	12.0	115791				
N	1.4	10499				
O	2.4	17964				
P	4.6	34151				
Q	0.8	7509				
R	197.9	2.99E6	1	20:17:46.7	+38:02:00.3	277[a]
			2	20:17:46.9	+38:02:01.9	29
			3	20:17:47.2	+38:02:04.7	28
			4	20:17:46.9	+38:02:02.2	23
			5	20:17:47.1	+38:02:06.6	21
			6	20:17:47.1	+38:02:04.2	21
			7	20:17:47.1	+38:02:06.5	20
			8	20:17:47.3	+38:02:03.7	20
			9	20:17:47.0	+38:02:05.8	19
			10	20:17:47.0	+38:01:52.7	18
			11	20:17:46.7	+38:02:05.1	14
			12	20:17:47.6	+38:02:03.3	14
			13	20:17:47.5	+38:02:04.4	14
			14	20:17:47.4	+38:02:06.8	13
			15	20:17:46.6	+38:01:50.3	12
			16	20:17:46.9	+38:02:04.7	12
			17	20:17:46.7	+38:02:04.2	11
			18	20:17:46.6	+38:01:51.8	10

[a] Very likely a background sources

3.1 Astrometry

To improve the transformation from image coordinates in pixel to astronomical RA and DEC we searched for astrometrically calibrated images in the available databases and we found several Wide Field and Planetary Camera 2 (WFPC2) images taken with F658N filter. Then, we identified on the image built by co-adding the retrieved images several faint stars surrounding P Cygni. The same stars were searched on our images and their positions were used in *ccmap* and in *ccsetwcs* IRAF tasks to add a World Coordinate System (WCS) to each of our individual frames. Eventually, the 72 frames were combined with the *imcombine* IRAF task to create a merged/collaged *Comb* image and a σ–image covering about an almost circular field of view of about $23''$ in radius with a central vignetting of about $1''$. Both images have astrometric accuracy on the order of $\pm 0''.15$ as derived by the

residuals of the position fit in *ccmap*. The *Comb* image is shown, in arbitrary intensity scale, in Fig. 1 with superimposed circles marking the positions of the comparison stars derived from the WFPC2 image. It is clearly evident that the scatter light of the P Cygni Point Spread Function (PSF) dominates and must be removed before investigating the nebular emission. As far as the angular resolution of the *Comb* image is concerned the analysis of the comparison stars indicate an average FWHM of about $0''.08$ confirming that the LBT AO system was able to achieve diffraction limit quality in the [Fe II] λ=1.6435 μm filter.

Assuming a circular symmetric PSF, we computed radial profiles of P Cygni scatter light distribution at different azimuth angles $\theta_{\rm i}$. The hypothesis of circular symmetry was then checked by over-plotting pairs of radial profiles at $\theta_{\rm i}$ and $\theta_{\rm i} + \pi$ (see some examples in Fig. 2). Finally, the distributions of intensity of the radial profiles at different distances, R, from the nominal position of P Cygni were built and analyzed leading to, for each R, at the determination of the intensity of the mean angular radial profile of the scattered light. To do this, we assumed that the minimum (after removing a few clear outliers) of the distribution of intensity at each radial distance is not affected by a significant nebular emission. We were able to derive a reliable radial profile only in an annulus around P Cygni position characterized by an inner and an outer radius of $R = 3''$ and $R = 19''$ respectively. In fact, at $R < 3''$ there is practically no pair ($\theta_{\rm i}$, R) where a contribution of nebular emission can be excluded *a priori*, while at $R > 19''$ the radial profiles are very noisy due to the reduced number of overlapping individual frames used to obtain the *Comb* image at these distances from P Cygni and to the intrinsic low signal in each individual frame.

The image of the nebular emission, *Neb*, was eventually obtained by subtracting the above–described scattered light model from the *Comb* image and it is shown in Fig. 3.

4 RESULTS

By comparing the intensity levels of the *Neb* image with those of the σ–image, we were able to identify in the former several nebular emission regions in the [Fe II] line at λ=1.6435 μm (labeled in Fig. 4) which can be defined as those close regions characterized by an Signal–to–Noise Ratio (S/N) greater than 3. In Table 1 we report, for each region, its size and total intensity within its boundary defined by the S/N=3 threshold, and the positions and the intensity of its emission maxima (knots). As can be seen in Fig. 4 most of the emission regions are consistent with the finding by Smith & Hartigan (2006) which stated, on the bases of

radial velocity measurements, that inner–shell of the P Cygni nebula can be approximated with a spherical shell characterized by an inner an outer radius at a distance of $R = 7''.8$ and $R = 9''.7$, respectively. Our results are also in relatively good agreement with the image in [N II] λ6584 of the inner–shell found by Barlow et al. (1994) even if we do not find a larger diameter in the North–South direction than in the East–West direction. On the other hand, our results show clearly the presence of extended emission also inside $R = 7''.8$ and outside $R = 9''.7$ with some asymmetry due to stronger emission at North–Northwest than at South–East of P Cygni. There are also hints of emission regions at larger radial distances, i.e. $R > 16''$ and of some possible connection with the internal regions in the North–West (see region R in Fig. 4). While we are very confident on the results we obtained for $R \leqslant 15''$ we must point out that for larger R we have the co–addition of only few individual frames and larger uncertainties on the subtracted average radial profile of P Cygni scattered light. Thus, the presence of a second region of nebular emission at the border of our field of view would require more dedicated observations to be soundly confirmed.

A direct comparison of our results with those already reported in the literature can be done by superimposing over the *Neb* image the *Spex* (red box in Fig. 5) and the three *CSHELL* long slits (blue, green, and magenta boxes in Fig. 5) used in the paper by Smith & Hartigan (2006).

By integrating in RA the *Neb* image counts contained in the *Spex* slit region we obtained Fig. 6 which can be compared with top panel of Fig. 4 by Smith & Hartigan (2006). As can be seen, there is a general agreement between our results and those previously reported by Smith & Hartigan (2006). It is also very clear, by comparing the upper and the lower panel, the gain in spatial resolution we achieved by taking advantage of the LBT AO system. It is worthwhile noticing that our integrated counts contains not only the nebular emission at the [Fe II] line at λ=1.6435 μm but, actually, the whole nebular emission in the filter wavelength band, thus including also some contribution from the weak nebular continuum. This continuous emission, which can be seen in third panel of Fig. 3 by Smith & Hartigan (2006), can explain why our integrated counts in the lower panel of Fig.6 do not go to zero at a distance of about 15″ East or West from P Cygni RA as in Fig. 4 by Smith & Hartigan (2006).

As far as the *CSHELL* slits are concerned, the integration in DEC of the *Neb* image counts should be compared with Fig. 5 by Smith & Hartigan (2006) taking into account that we do not have radial velocity information. In any case, there is a qualitative agreement

since the maxima in the right panels of Fig. 7 fall at the same DEC of the knots in Fig. 5 by Smith & Hartigan (2006). It is clear that the intensity of the different maxima in Fig. 7 are the results of co–adding the emission of nebular regions along the line of sight characterized by different radial velocities. The same effect is obviously present in Fig.s 3–6 showing that to derive the actual 3–D mapping of the inner–shell of P Cygni nebula we have to wait until complete coverage in both imaging and radial velocity will be available.

5 FUTURE OBSERVATIONS

With the aim of deriving a full 3–D picture of the inner–shell of PCygni nebula, we aim to obtain NIR spectra in the wavelength region of the strongest [Fe II] nebular lines to discriminate in our image the approaching and the receding parts of the ejecta by measuring their radial velocities. These spectroscopic measurements, together with our 2–D image, will allow us to use a more detailed geometry and a more constrained filling factor value than those used by Smith & Hartigan (2006), to derive more reliable and accurate estimate of the ejecta mass. Furthermore, the radial velocity measurements in the regions at radial distances larger than $10''$ might allow us to get hints on the dates of ejection episode(s) that occurred before the 1600 AD outburst. In such a way we could estimate the typical time period between such eruptions which is needed in order to understand how much of the mass loss, which causes a massive stars to become a Wolf–Rayet star, occurs in giant brief eruptions.

In conclusion, it is also worthwhile noticing that it could be feasible to measure the expansion proper motions of the inner–shell of P Cygni nebula starting from the high spatial resolution ($0''.08$) image presented in this paper by obtaining, in the near future, new NIR AO images. In fact, assuming a constant expansion velocity of $\sim$140 km/s and a distance of 1.7 kpc, it would be possible to resolve the apparent motion of the brightest emission knots after an elapsing time of less than 10 years.

ACKNOWLEDGMENTS

We acknowledge the support from the LBT-Italian Coordination Facility for the execution of observations, data distribution and reduction.

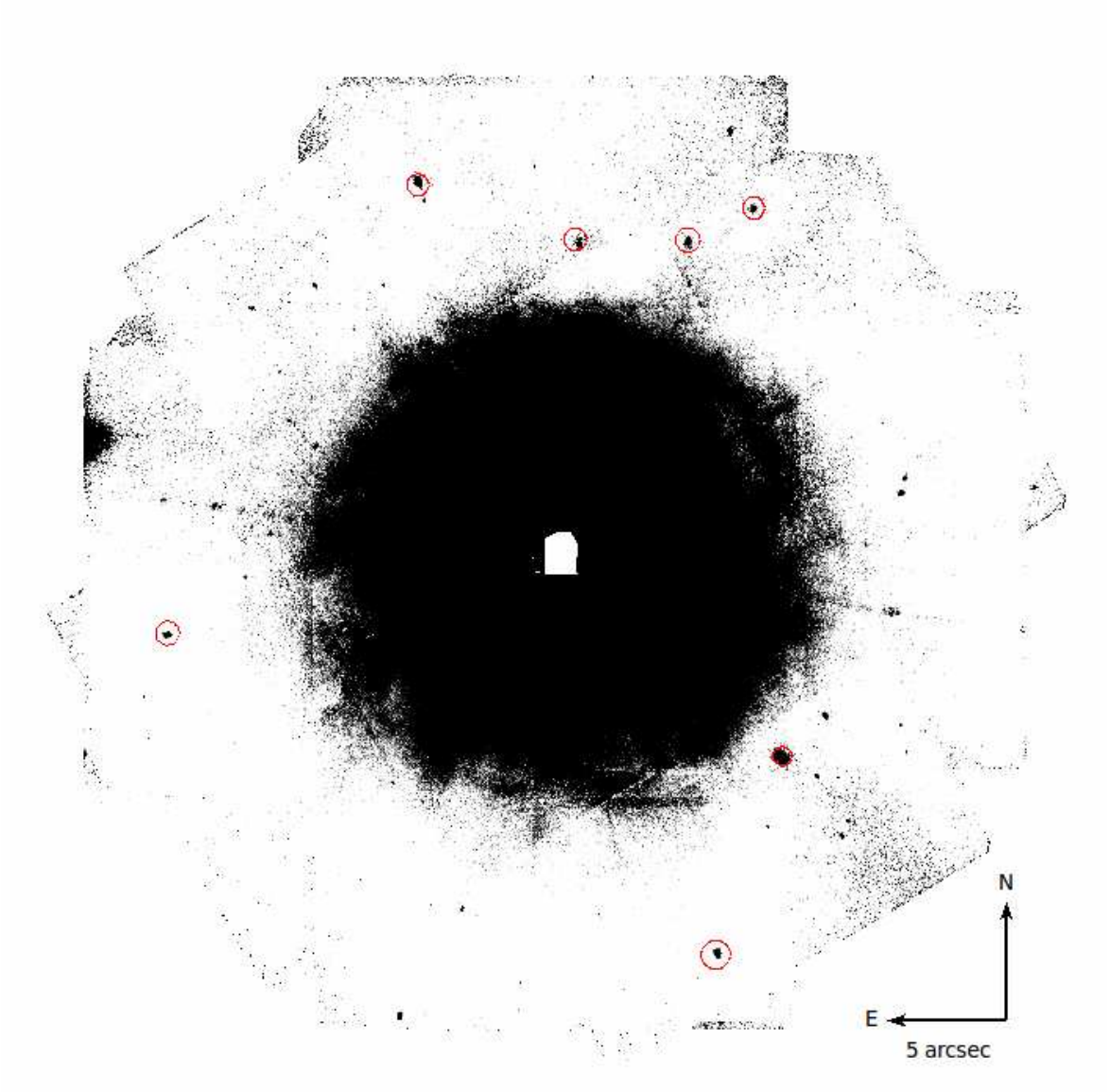

Figure 1. *Comb* image in the [Fe II] nebular emission line of the inner–shell of the P Cygni nebula. The superimposed red circles are centered on the centroid positions of the comparison stars in the WFPC2 image.

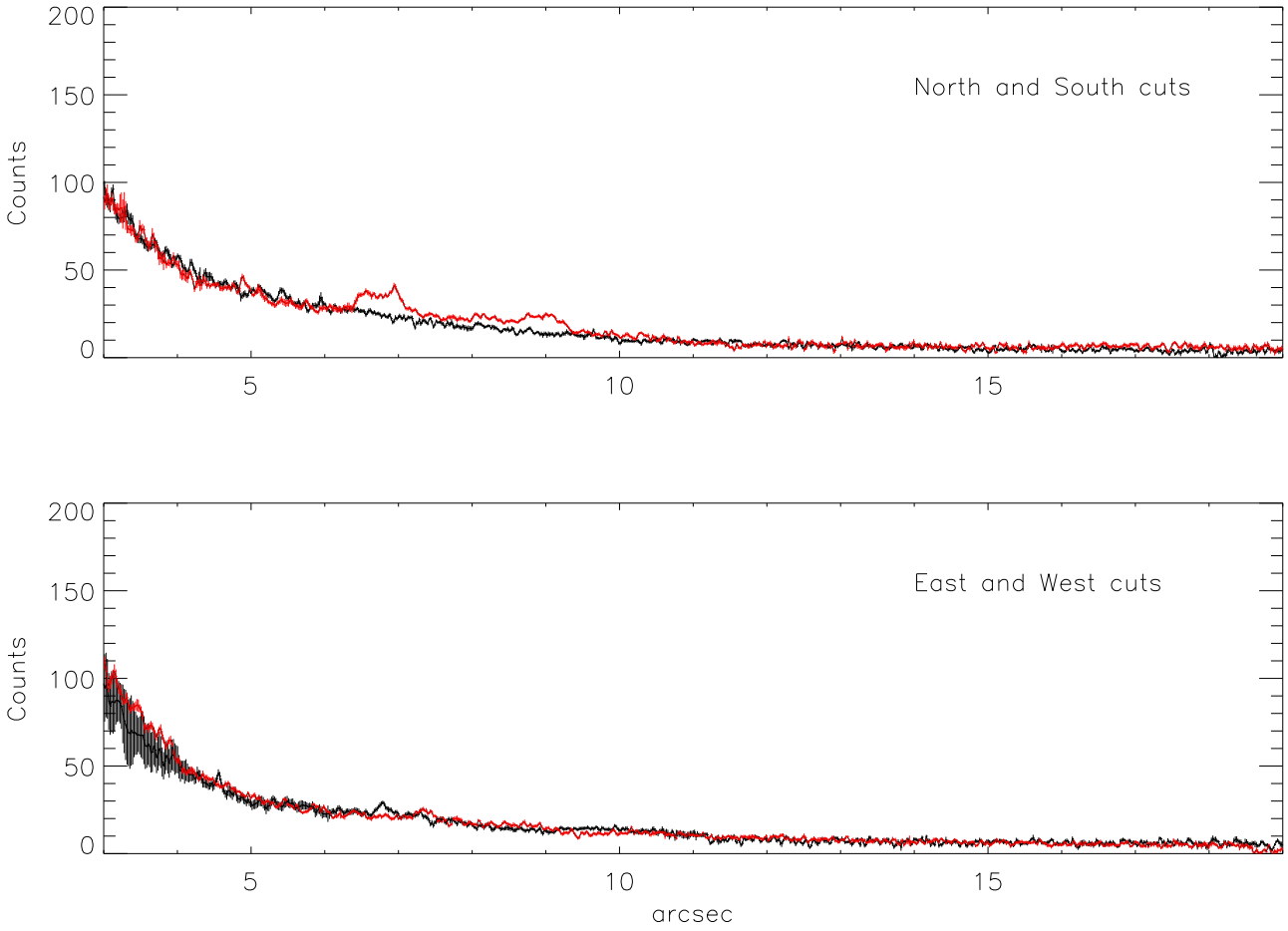

Figure 2. *Comb* image cuts starting at nominal P Cygni position. Upper panel: towards South (black, $\theta = \pi$) and towards North (red, $\theta = 0$); lower panel: towards East (black, $\theta = 3/2\pi$) and towards West (red, $\theta = \pi/2$). The excesses of counts at distances of about $R = 7''$ and $R = 9''$ from P Cygni position in the red cut of the upper panel with respect to the black one are due to nebula emission regions (see Fig. 4 and Sec. 4)

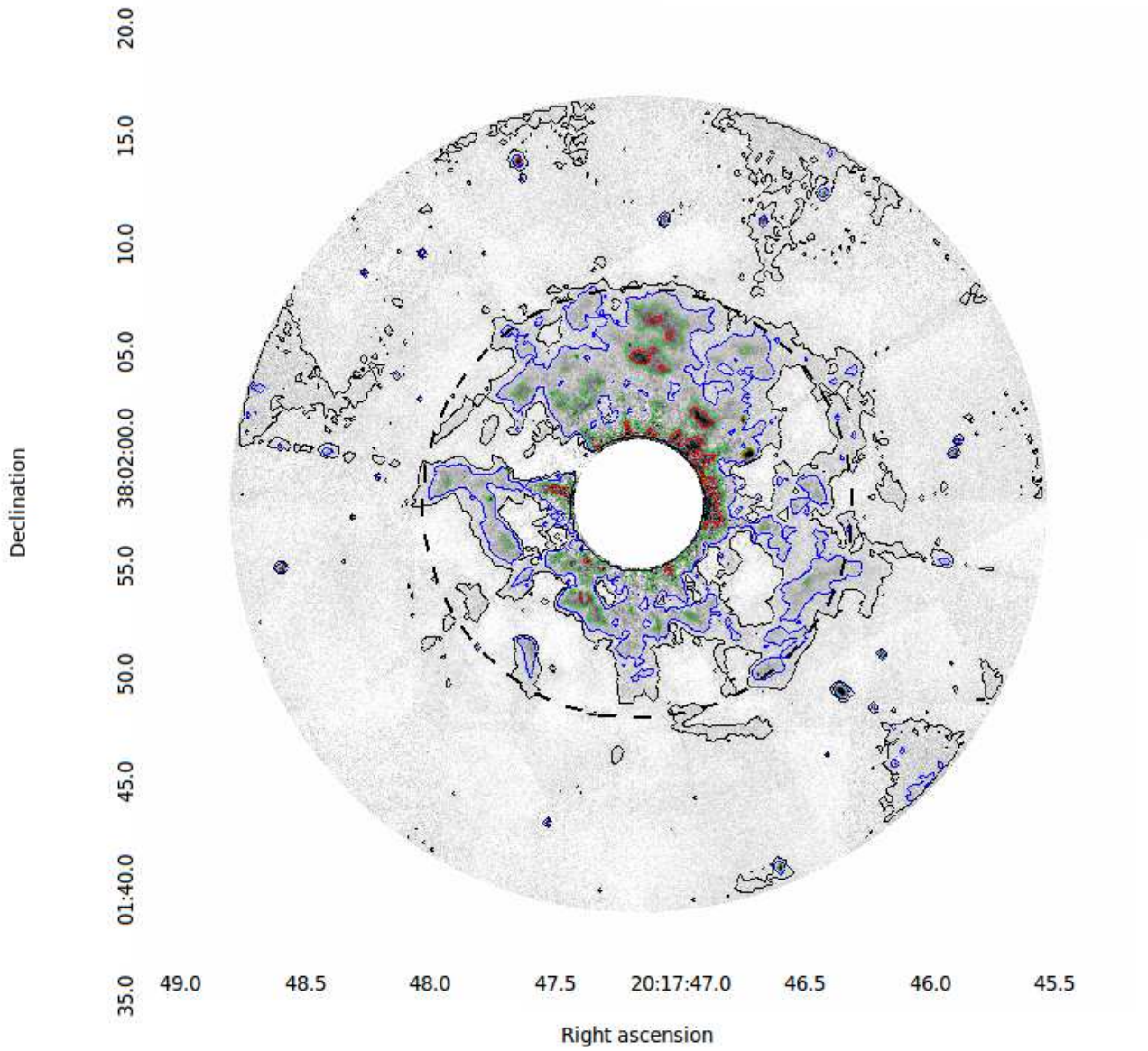

Figure 3. *Neb* image of the inner–shell of the P Cygni nebula, obtained by subtracting from *Comb* image a model of P Cygni scattered light built using an average radial profile (see text), with superimposed intensity contour levels at 3 (black), 5 (blue), 10 (green), and 15 (red) counts. The radius of the dashed black circle is 10″.

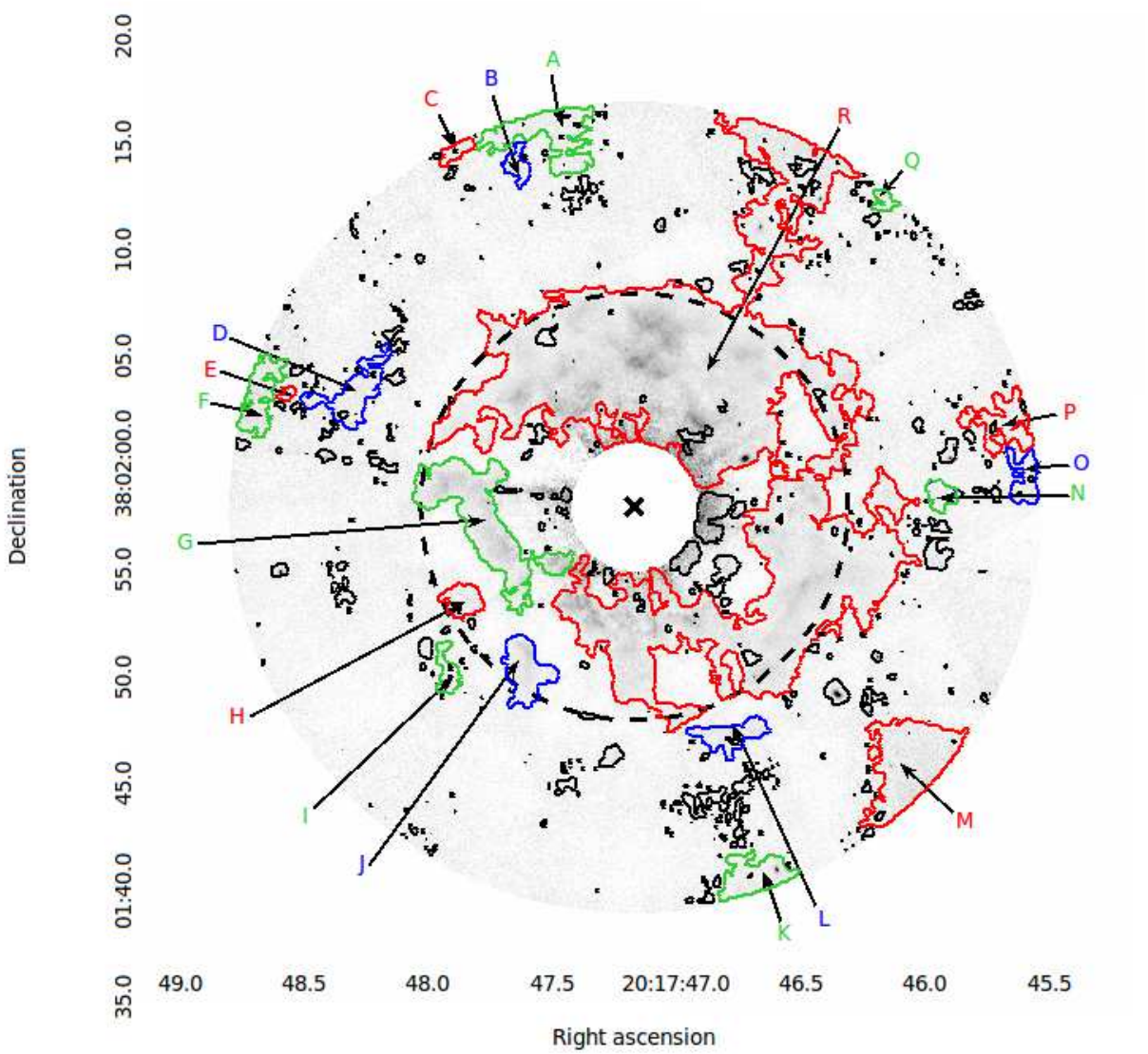

Figure 4. Most prominent [Fe II] emission regions in the inner–shell of the P Cygni nebula defined as closed areas within S/N=3 boundary. Main parameters of each area identified by an alphabetic character can be found in Table 1. The position of P Cygni is indicated by "X" symbol, the radius of the dashed black circle is $10''$.

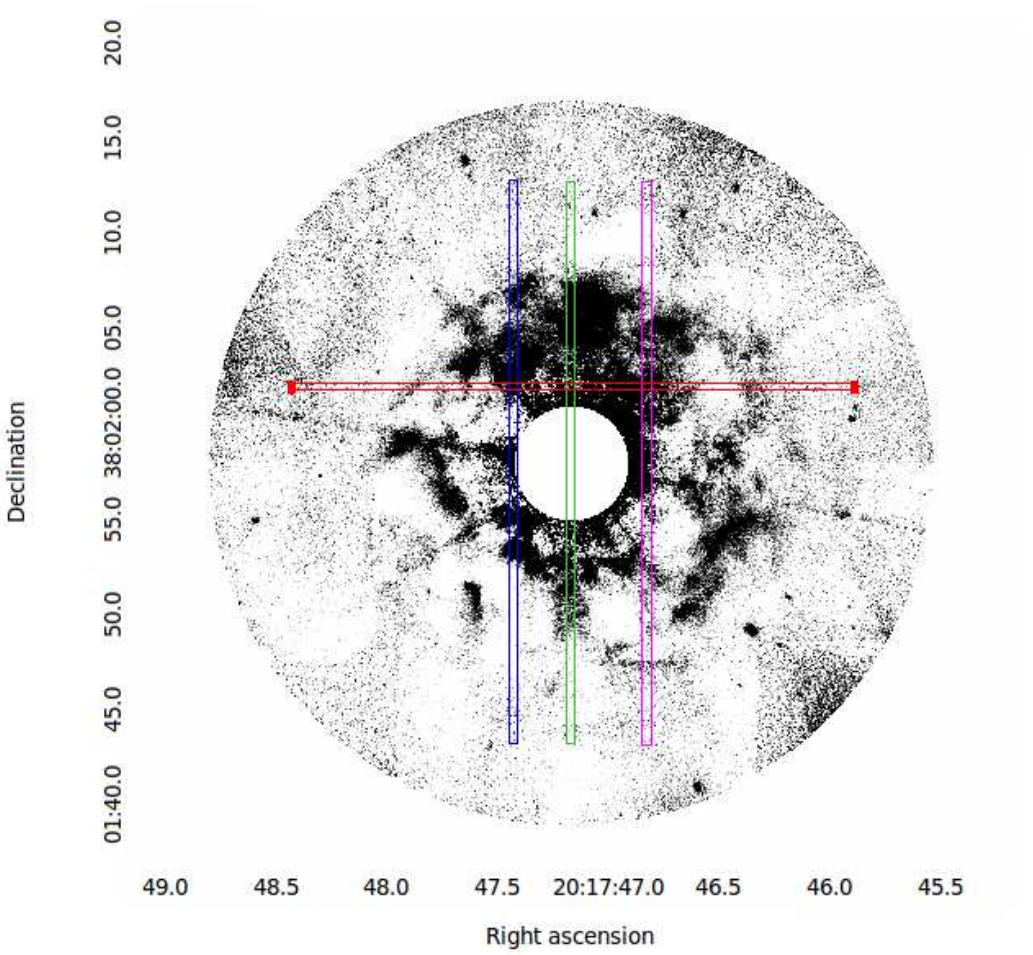

Figure 5. Long slits used in the paper by Smith & Hartigan (2006) superimposed over *Neb* [Fe II] image of the inner–shell of P Cygni nebula (see text).

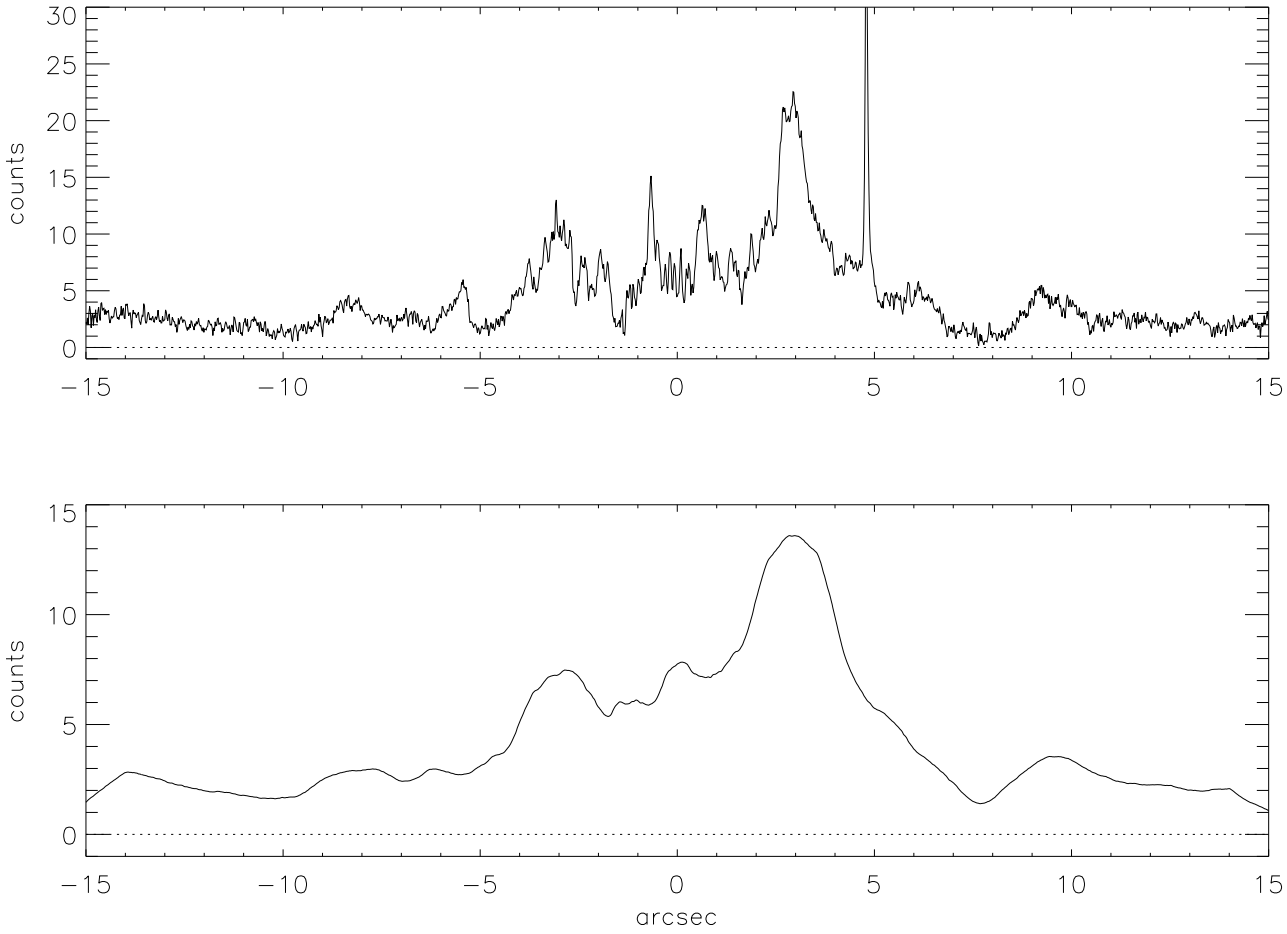

Figure 6. [Fe II] emission intensity in the East-West area (red box in Fig.5) 0″.3 wide centered at 4″ north of the inner–shell of the P Cygni nebula. Upper panel: the original data in the [Fe II] nebular emission line (the peak at 4″.9 West is due to a background source); lower panel: original data degraded at 2″ spatial resolution to mimic upper panel of Fig. 4 by Smith & Hartigan (2006) after removing the background source.

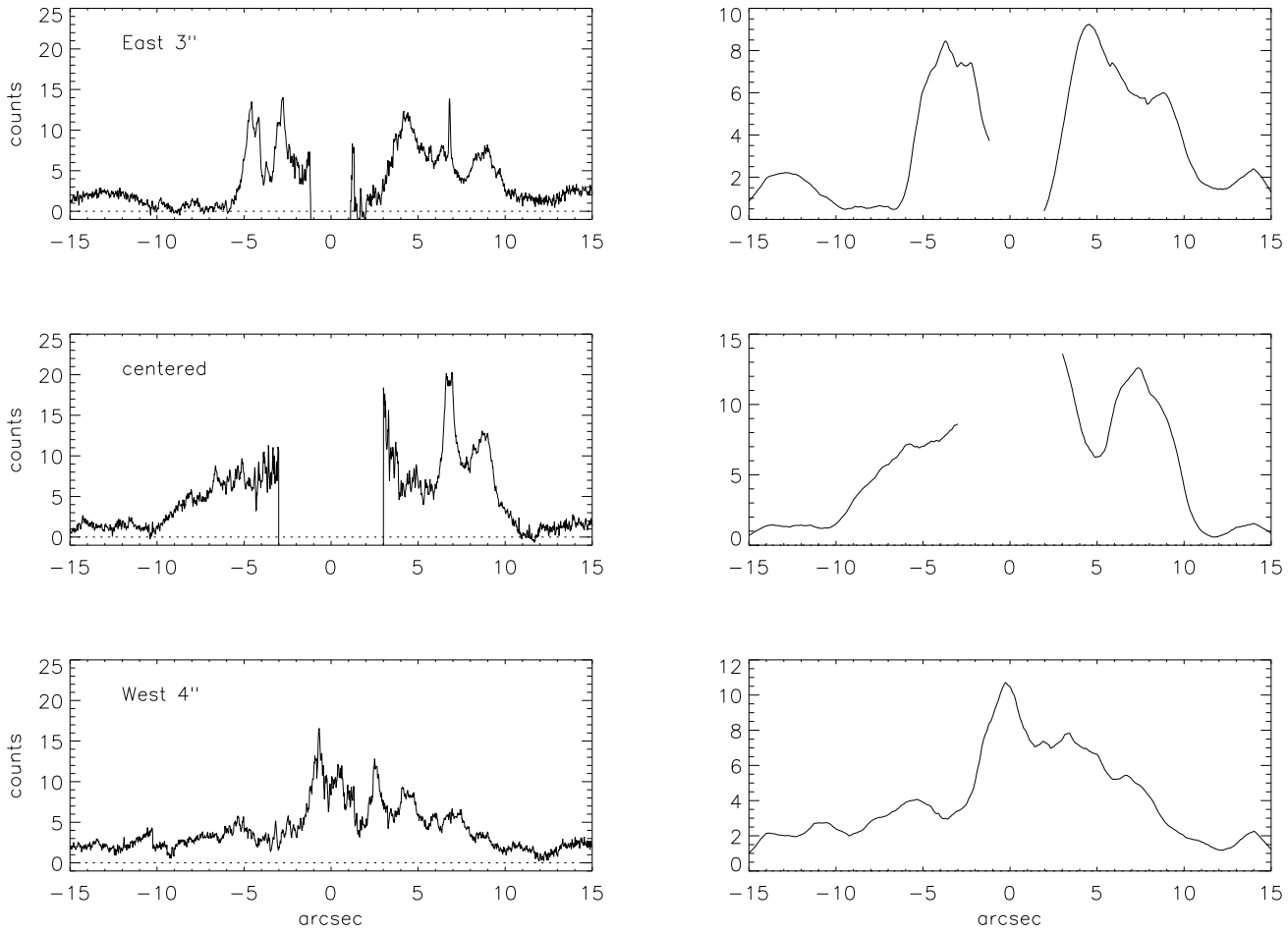

Figure 7. [Fe II] emission intensity in the South-North areas (blue, green, and magenta boxes in Fig.5) 0″.5 wide centered at 3″ East of P Cygni (upper panels), on star (middle panels), and at 4″ West of P Cygni (lower panels). Left panels: original data; right panels: original data degraded at 2″ spatial resolution to mimic Fig. 5 by Smith & Hartigan (2006).

REFERENCES

Barlow, M.J., Drew,J. E. Meaburn, J., Massey,R.M., 1994, MNRAS, 268, L29

Esposito, S. et al., 2012, in Adaptive Optics Systems III Proceedings of the SPIE, 8447, 84476B

Esposito, S. et al., 2013, A&A, 549, A52

Guerra, J., Boutsia, K., Rakich, A., et al. 2012, PISCES Technical Report

Hill, J. M., 2010, Appl. Opt., 49, D115

Latherer, C., Zickgraf, F.J., 1987, A&A, 174, 103

McCarthy et al., 2001, PASP, 113, 353

Meaburn, J., Lopez, J. A., Barlow, M. J., Drew, J. E., 1996, MNRAS, 283, L69

Meaburn, J., Lopez, J. A., O'Connor, J. A., 1999, ApJ, 516, L29

Meaburn, J., Boumis, P., Redman, P., Lopez, J. A., Mavromatakis, F., 2004, A&A, 422, 603

Najarro, F., 2001, in ASP Conf. Ser. 233, P Cygni 2000: 400 Years of Progress, ed. M. de Groot & C. Sterken (San Francisco, CA: ASP), 131

Najarro, F., Hillier, D. J., Stahl, O., 1997, A&A, 326, 1117

Nota A., Livio M., Clampin M., 1995, ApJ, 448 788

Ragazzoni, R., 1996, Journal of Modern Optics, 43, 289

Riccardi, A. et al., 2010, in Adaptive Optics Systems II Proceedings of the SPIE, 7736, 77362C

Salinari, P., del Vecchio, C., Biliotti, V., 1993, in Proceedings of the ICO-16 Conference on Active and Adaptive Optics, 247

Smith, N. 2001, in ASP Conf. Ser. 233, P Cygni 2000: 400 Years of Progress, ed. M. de Groot C. Sterken (San Francisco: ASP), 125

Smith, N., Hartigan, P., 2006, ApJ, 638, 1045

White, R. L., Becker, R.H., 1982, ApJ, 262, 657

This paper has been typeset from a TEX/ LATEX file prepared by the author.